THE JOURNAL OF PHYSICAL CHEMISTRY A
A JOURNAL OF THE AMERICAN CHEMICAL SOCIETY

pubs.acs.org/JPCA Article

Role of the Solvent and Intramolecular Hydrogen Bonds in the Antioxidative Mechanism of Prenylisoflavone from Leaves of *Vatairea guianensis*

Sávio Fonseca, Neidy S. S. dos Santos, Alberto Torres, Marcelo Siqueira, Antônio da Cunha, Vinícius Manzoni, Patricio F. Provasi, Rodrigo Gester,* and Sylvio Canuto

Cite This: *J. Phys. Chem. A* 2023, 127, 10807−10816

Read Online

ACCESS | Metrics & More | Article Recommendations

ABSTRACT: This work discusses the electron structure, antioxidative properties, and solvent contribution of two new antioxidant molecules discovered, named **S10** and **S11**, extracted from a medicinal plant called *Vatairea guianensis*, found in the Amazon rain-forest. To gain a better understanding, a study using density functional theory coupled with the polarizable-continuum model and the standard 6-311++G(d,p) basis set was conducted. The results indicate that **S10** has a higher antioxidant potential than **S11**, confirming the experimental expectations. In the gas phase, the hydrogen atom transfer route dominates the hydrogen scavenging procedure. However, in the water solvents, the antioxidant mechanism prefers the sequential proton loss electron transfer mechanism. Furthermore, the solvent plays a fundamental role in the antioxidant mechanism. The formation of an intramolecular OH···OCH_3 hydrogen bond is crucial for accurately describing the hydrogen scavenging phenomenon, better aligning with the experimental data. The results suggest that the two isoflavones investigated are promising for the pharmacologic and food industries.

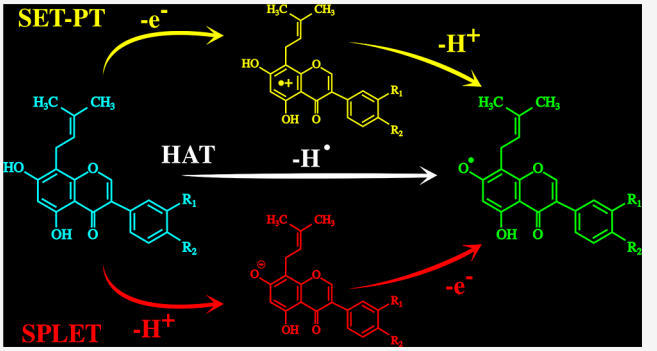

1. INTRODUCTION

Free radicals are harmful substances produced naturally in living organisms during the burning of oxygen necessary to convert nutrients into energy. These radicals can damage healthy cells, causing premature aging of the human organs and skin tissues in humans.[1,2] However, living organisms have enzymes that regulate metabolism and can repair up to ca. 99% of the damage produced by these free radicals. However, poor diet, smoking, alcohol abuse, and even excessive physical exercise are everyday factors that can break this balance.

Consumption of species with antioxidant functions becomes fundamental for maintaining a healthy life. An antioxidant is an organic substance prone to hydrogen dissociation that eliminates a free radical. For these reasons, these flavonoids are widely used in the cosmetic, food, and pharmacological industries, for example, preventing early aging, some cancers, and cardiovascular and respiratory diseases.[2−6]

The discovery of new compounds typically involves extraction from natural products and careful biological assays. However, molecular modeling techniques associated with quantum mechanical methods have made relevant contributions in this direction.[7−18] From a theoretical point of view, there are three mechanisms in which hydrogen scavenging can occur, that is by which the antioxidant (ArOH) donates hydrogen to the free radical $X^{\bullet}$: hydrogen atom transfer (HAT), sequential proton loss electron transfer (SPLET), and sequential electron transfer-proton transfer (SET-PT).[19,20] Figure 1 shows this mechanism, which is represented respectively

1. Hydrogen atom transfer

$$ArOH + X^{\bullet} \rightarrow ArO^{\bullet} + XH \quad (1)$$

2. Sequential proton loss electron transfer.

$$ArOH \rightarrow ArO^{-} + H^{+} \quad (2)$$

$$ArO^{-} + X^{\bullet} + H^{+} \rightarrow ArO^{\bullet} + XH \quad (3)$$

3. Sequential electron-transfer and proton-transfer.

$$ArOH + X^{\bullet} \rightarrow ArOH^{\bullet+} + X^{-} \quad (4)$$

$$ArOH^{\bullet+} + X^{-} \rightarrow ArO^{\bullet} + XH \quad (5)$$

Received: August 24, 2023
Revised: December 4, 2023
Accepted: December 6, 2023
Published: December 18, 2023

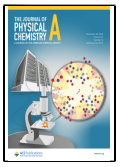

https://doi.org/10.1021/acs.jpca.3c05725
J. Phys. Chem. A 2023, 127, 10807−10816

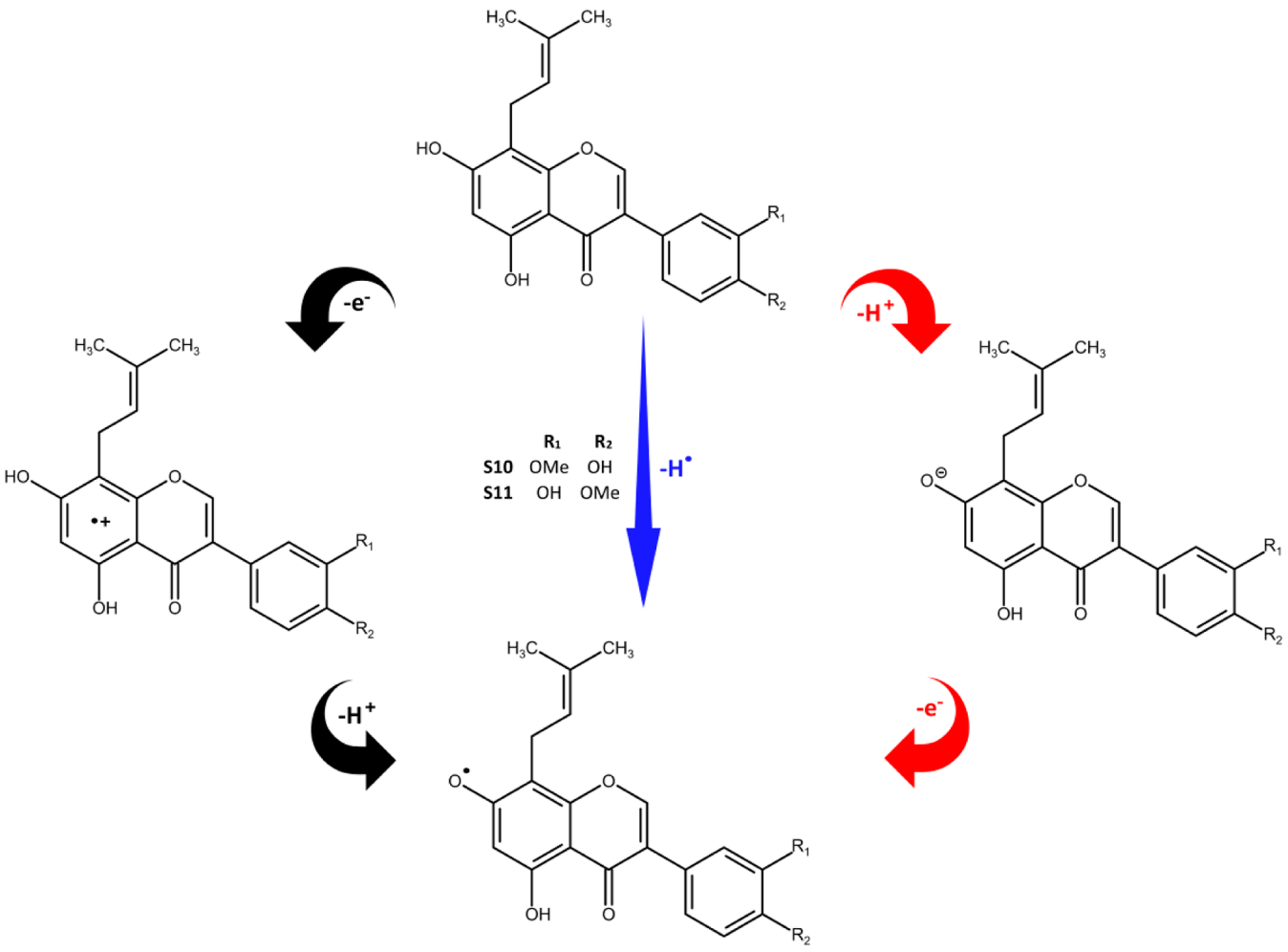

Figure 1. Antioxidant effects of prenylisoflavones through the following mechanisms: HAT (blue), SPLET (red), and SET-PT (black color).

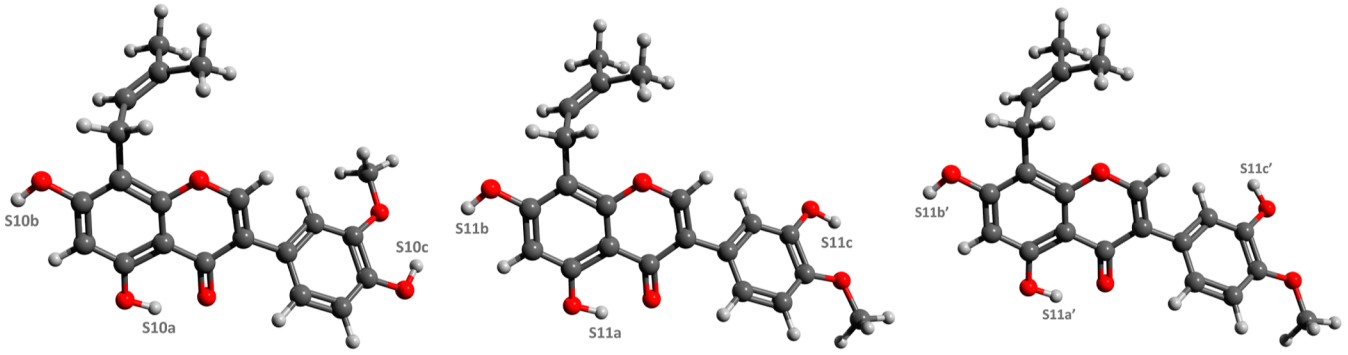

(a) **S10** (b) **S11** (c) **S11'**

Figure 2. Molecular structures of the two prenylisoflavones: **S10** (5,7,4′-trihydroxy-3′-methoxy-8-prenylisoflavone) and **S11** (5,7,3′-trihydroxy-3′-methoxy-8-prenylisoflavone). **S11′** is another geometry of minimum energy obtained for molecule **S11**. The hydroxyl hydrogen at **S11c′** is not bonded to the methoxy group. The chemical elements are white (hydrogen), gray (carbon), and red (oxygen).

It is experimentally unfeasible to verify all of the details of the hydrogen dissociation mechanism. However, quantum mechanics theory makes it possible to "see and follow" all the stages of these mechanisms, determining the best route for hydrogen scavenging and all the factors that influence it and, therefore, obtain the antioxidant behavior of a compound. The hydrogen scavenging is composed of a sequence of quantum mechanical transition states. However, the theory of thermodynamics says that only the thermochemical parameters corresponding to the initial and final state are relevant.[21] Hence, these goals are obtained simply by applying quantum chemistry methodologies to acquire the enthalpies (H) at different points in these processes. This strategy allows determining the structure and the most favorable antioxidant mechanism in gas or solution since the solvent can affect the form of hydrogen scavenging.[22−25]

Antioxidants are natural products found in many plant species and edible fruits, a relevant branch of Organic Chemistry.[26] Flavonoids constitute an interesting case of study. These

https://doi.org/10.1021/acs.jpca.3c05725
J. Phys. Chem. A 2023, 127, 10807−10816

compounds comprise a class of phenolic compounds that regulate various functions essential to plant life. In human organisms, flavonoids show benefits for health, e.g., outstanding antioxidant behavior.[27−30] Therefore, the pharmacological activities of these compounds have been studied and evidenced in research.

In the search to map the biological potential of the Amazon biome, recent work has measured ^{1}H and ^{13}C nuclear magnetic resonance as well as ultraviolet−visible spectroscopy to characterize and report a new prenylisoflavone derivative in *Vatairea guianensis*[31] leaves. In addition to the compound 5,7,4′-trihydroxy-3′-methoxy-8-prenylisoflavone (**S10**), this work has mentioned a novel compound called 5,7,3′-trihydroxy-3′-methoxy-8-prenylisoflavone (**S11**). These two compounds (Figure 2) are of interest because they are positional isomers having chromone and phenolic groups in which the hydroxyl and methoxy termini can reduce free radicals in the human organism. Preliminary discussion has indicated that among the seven compounds extracted from the plant *V. guianensis*, only species **S10** and **S11** exhibited significant free radical scavenging activity.[32] The results indicate that isoflavone **S10** would be a more accessible compound for hydrogen absorption processes. However, nothing is known about the hydrogen elimination pathway, which is problematic as the environment can easily change this mechanism from gas to solvent.[15,64] The differences in antioxidant potentials are expected to remain at the phenolic end since the compounds are positional isomers.

For the first time, a systematic quantum chemical investigation of the oxidative mechanism of these two flavonoids is carried out. The discussion is based on a density functional theory (DFT)[33−35] analysis of the electron structure and thermochemical energies involved in the three hydrogen dissociation mechanisms (HAT, SPLET, and SET-PT). Although both species have structures very similar, intramolecular hydrogen bonds (HBs), OH···OCH_3, and solute−solvent interactions determine the antioxidant behavior.

2. METHODOLOGY

All structural and energy analyses were carried out within the DFT[33−35] framework using the ωB97XD functional[36] and the standard 6-311++G(d,p) basis set[37,38] in the gas phase environment. The polarizable continuum model (PCM), with water dielectric, was applied according to the integral equation formalism.[39] As standard, the restricted functional ωB97XD, which uses a version of the Grimme dispersion model, was applied for neutral and monoionic structures, and the unrestricted method was used to deal with radicals and radical cations.19 The geometries corresponding to the local minimum energies were tested after the infrared spectra were analyzed and verified that all calculated vibrational frequencies were positive.

Numerical parameters related to hydrogen up-taking have been previously reported,[15,19,20] and according to such works, bond dissociation enthalpy (BDE−HAT mechanism) should be considered as an antioxidant parameter

$$BDE = H^{\bullet}_{ArO} + H^{\bullet}_{H} - H_{ArOH} \quad (6)$$

Proton affinity and electron transfer enthalpy (PA and ETE SPLET mechanism)

$$PA = H^{-}_{ArO} + H^{+}_{H} - H_{ArOH} \quad (7)$$

$$ETE = H^{\bullet}_{ArO} + H_{e} - H^{-}_{ArO} \quad (8)$$

Adiabatic ionization potential and proton dissociation enthalpy (AIP and PDE SET-PT mechanism)

$$AIP = H^{\bullet+}_{ArOH} - H_{ArOH} + H_{e} \quad (9)$$

$$PDE = H^{\bullet}_{ArO} + H^{+}_{H} - H^{\bullet+}_{ArOH} \quad (10)$$

In this context, we have the enthalpies of the compound (H_{ArOH}), anion (H^{-}_{ArO}), radical ($H^{\bullet}_{ArO}$), radical cation ($H^{\bullet+}_{ArOH}$), a hydrogen atom ($H^{\bullet}_{H}$), proton (H^{+}_{H}), and electron (H_e), where all the quantum mechanical calculations were performed using Gaussian 09.40 Table 1 presents the enthalpies needed to calculate the HAT, SPLET, and SET-PT mechanisms. The enthalpies of protons and electrons have been used for the enthalpy of the hydrogen. This topic has been extensively discussed previously using established basis set extrapolated DFT and coupled cluster calculations, and the estimated results for the DFT-B3LYP method (−1309.85 to −1312.93 kJ/mol)[41,42] are also in good agreement with values obtained in this work.

Table 1. Previously Reported Reference Values19 for the Enthalpy of the Hydrogen Atom, Proton, and Electron in the Gas Phase and Water

	enthalpy (kJ/mol)	
compound	gas phase	water
proton (H_H^+)	6.2	−1083.8
hydrogen atom ($H^{\bullet}_H$)	−1306.6	−1310.6
electron (H_e)	3.1	−101.9

3. RESULTS

3.1. HAT Mechanism. After a complete geometric optimization, **S10** and **S11**, as well as their radical anions and radical cations, were found to be in local minimum energy states, which were confirmed by the absence of imaginary frequencies in the vibration spectra; the more stable structures (see Figure 2) indicate that all hydroxyl moieties are involved in the formation of intramolecular HBs.[43]

One advantage of molecular modeling over experimental procedures is the fact that the electron structure of the material itself can provide information about which part of the molecule would be involved in the antioxidation process. For example, the topology and location of the HOMO (highest occupied molecular orbital) indicate the region most likely to lose the hydrogen atom in the scavenging procedure.[15,19] From Figure 3, it is possible to see that the HOMO plotted for the **S10** and **S11** molecules shows a high electron density in the phenol ring, indicating a tendency of OH to lose the hydrogen atom.

Another indirect and qualitative indicator of the radical formation is the SD calculated for the radicals formed, shown in Figure 3. The oxygen atom with the highest SD is the radical most likely to conform. For the **S11** molecule, for instance, the oxygen atom of the **S11c** radical presents an SD of 0.364, which is greater than those estimated for the other **S11a** (0.333) and **S11b** (0.352) molecules. Consequently, one expects that **S11c** is the most stable one. Similar results are obtained for the **S10** compound (Figure 4)

Theoretical knowledge is required to understand the protons, electrons, and hydrogen enthalpies in both gas and water. Figure 2 illustrates that both compounds contain CH_3, OCH_3, and OH groups capable of losing hydrogen and neutralizing free radicals. However, previous research indicates that the OH group is

https://doi.org/10.1021/acs.jpca.3c05725
J. Phys. Chem. A 2023, 127, 10807−10816

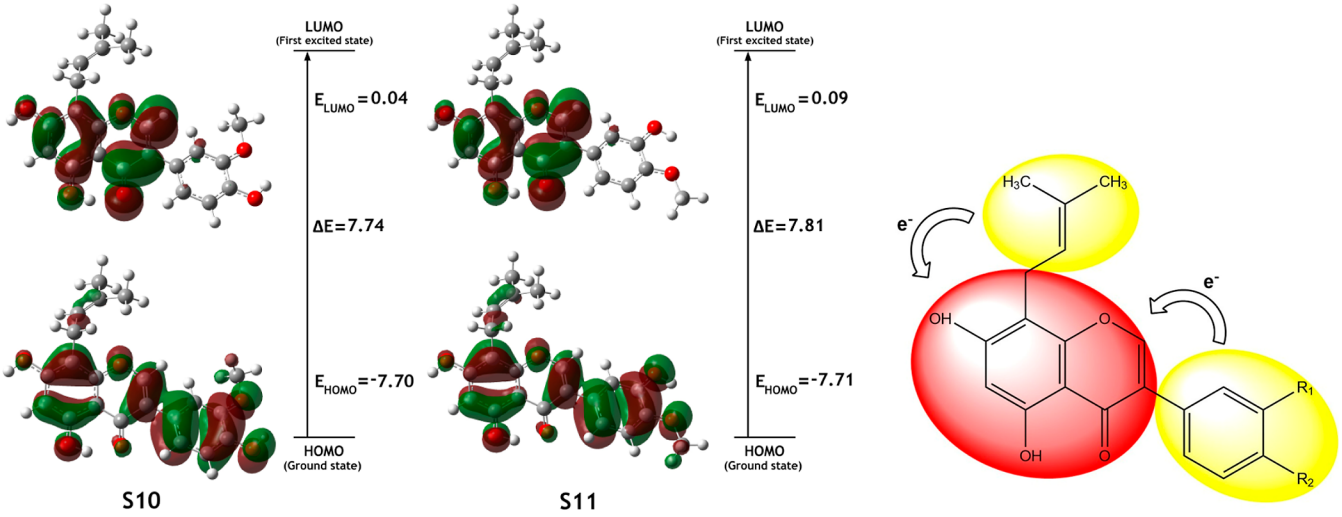

Figure 3. Frontier molecular orbitals (a) of S10 and S11 are calculated in the gas-phase using the level of approximation ωB97XD/6-311++G(d,p). In both molecules, the HOMO−LUMO transition indicates an intramolecular charge transfer (ICT) effect. On the right side, (b) schedule for the ICT process. Under gas-phase conditions, the charge variation on the red surface is $\Delta Q_{S10} = -0.142$ e and $\Delta Q_{S11} = -0.112$ e, respectively, considering the charges obtained for the ground state and the first excited state without relaxing the geometries of the molecules, which attests the charge gain.

energetically favorable for hydrogen removal.[32] Therefore, the molecular sites of interest are denoted as a, b, and c. To characterize the mechanism of HAT, Table 2 presents the results for BDE and $\Delta BDE = BDE_{molecule} - BDE_{phenol}$, which is defined using the phenol molecule as a reference. This last index is crucial to establish an efficient criterion for antioxidant behavior.

It is seen, upon investigation of the results on the specific molecular site under gaseous conditions, that the removal of hydrogen from position **S10a** requires 419 kJ/mol. This demand increases (373 kJ/mol) when the hydrogen atom is removed from position **S10b**. However, the results improve significantly (355 kJ/mol) for position **S10c**, indicating that this molecular site is most likely to lose the hydrogen radical. Also, compared to the phenol molecule, only the **S10c** site requires less energy, specifically, −6 kJ/mol. Furthermore, the antioxidant scale is **S10a** < **S10b** < **S10c**, which means that the **S10a** and **S10b** sites do not influence the hydrogen scavenging process.

The behavior is almost similar for **S11** molecule, a positional isomer of **S10**. From Table 2, it can be seen that the hierarchy is **S11a** < **S11b** < **S11c**, indicating that the position **S11c** is the path for hydrogen removal, requiring −5 kJ/mol less energy relative to phenol. However, de Souza et al.[32] have suggested that between the two compounds, **S10** exhibits better antioxidant behavior than **S11**. Quantum mechanical calculations in the gas phase support this trend, with **S10c** < **S11c** for the HAT mechanism at the ωB97XD/6-311++G(d,p) level of theory. Notice that although the BDE difference between the two isomers is small-scale, −6 and −5 kJ/mol for **S10c** and **S11c**, respectively, only one methoxyl and one hydroxyl group exchange positions within the same ring of the isomers. Therefore, the molecules have the same type of interactions and bonds, and their energetics are dominated by the balance between van der Waals dispersion and H-bonds, both of them very well described by ωB97XD (<1 kJ/mol).[36]

Before continuing, it is worth noting that the enthalpies of electrons, protons, and hydrogen were obtained using the B3LYP method, but it does not affect the predictions of ωB97XD. For example, after performing B3LYP calculations for the sites **S10c** and **S11c**, BDE values of 345 and 348 kJ/mol are obtained, which also indicates that the molecule **S10** is the best antioxidant compound. These results confirm the previous prediction of ωB97XD and are adopted here as the working method.

Another relevant aspect refers to the participation of the environment. According to the data presented in Table 2, aqueous dilution drastically reduces all BDE parameters but does not affect the other scale of antioxidants obtained in the gas phase, **S10a** < **S10b** < **S10c** and **S11a** < **S11b** < **S11c**. Furthermore, compared to phenol molecules, the solvent considerably improves the antioxidant performance of the compounds. For example, from gas to solvent, ΔBDE changes to −24 and −22 kJ/mol, respectively, for **S10c** and **S11c**.

Besides comparison with experimental results, an approach widely used to evaluate antioxidant efficacy is the DPPH (2,2-diphenyl-1-picrylhydrazyl) free radical inhibition assay. Antioxidant capacity is assessed by quantifying the percentage of the scavenging DPPH radical ($DPPH^{\bullet}$) and plotting it against the concentration of the sample. The resulting curve provides the IC_{50} value, which is the minimum concentration required to inhibit root activity by 50%. In summary, a lower IC_{50} value signifies a higher clearance activity and, consequently, a higher antioxidant capacity, providing evidence for the formation of DPPH-H during the reaction.[50,51] From Table 2, the molecule **S10** is the one that presents the lowest IC_{50} value, 72.2 ± 0.1 μg mL^{-1}, that corresponds to the highest value for the antioxidant performance, according to theoretical predictions.

Several studies have provided evidence for the synergy concept between species, particularly flavonoids, where their combined effects are greater than the sum of their individual effects.[52−54] This notion is based on the hypothesis that various compounds can target different components of oxidative systems, thus enhancing and complementing their overall activity. This synergy is realized in the leaf (6.2 ± 0.4 μg mL^{-1}) and the sapwood (3.7 ± 0.3 μg mL^{-1}) excerpts from *V. guianensis*, which are characterized by the lowest values for IC_{50}. Thus, the mixture of molecules **S10** and **S11** can improve antioxidant behavior.

https://doi.org/10.1021/acs.jpca.3c05725
J. Phys. Chem. A 2023, 127, 10807−10816

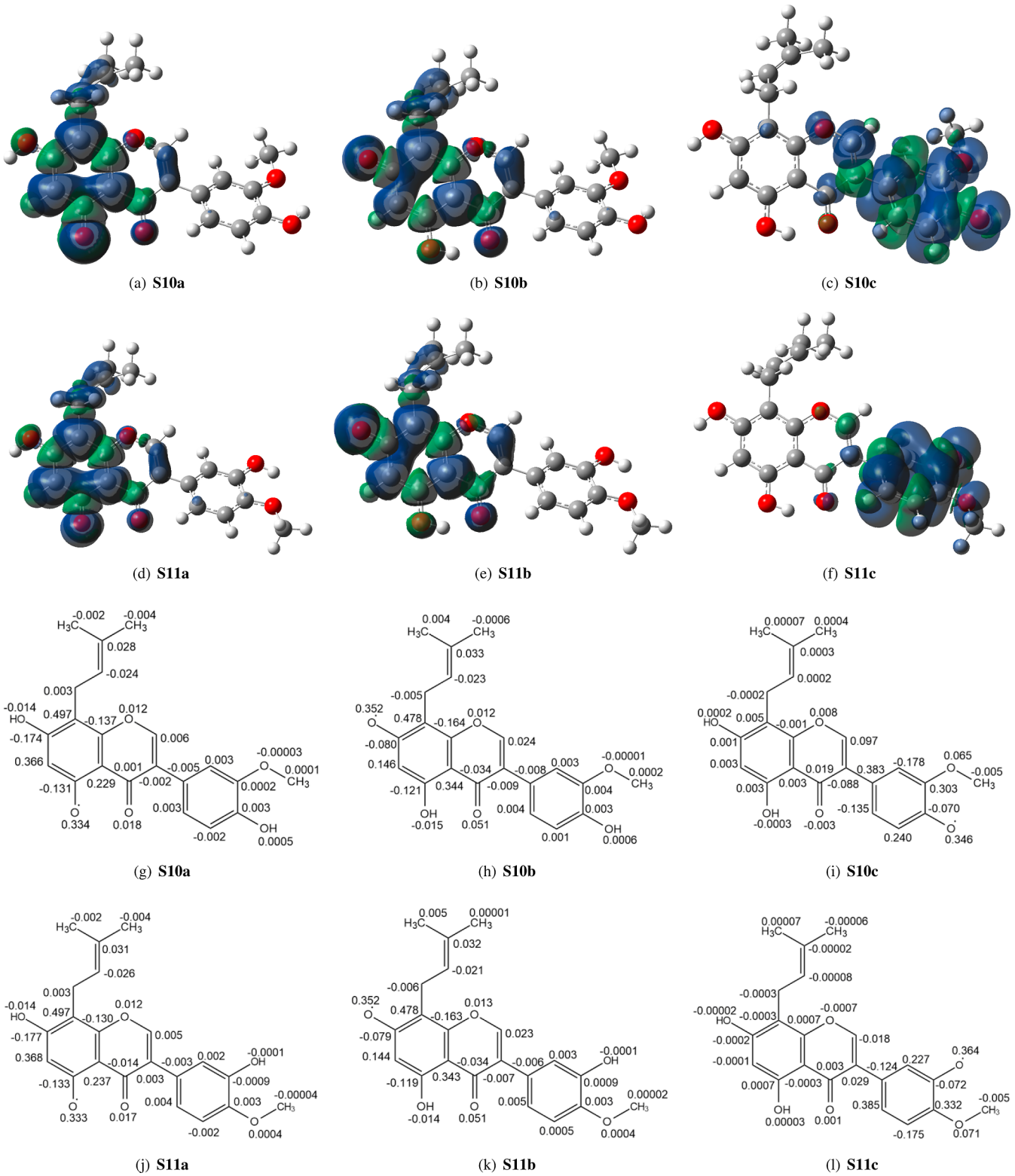

Figure 4. Plot (a–f) and numerical values (g–l) of unrestricted ωB97XD/6-311++G(d,p) total atomic spin densities distributions for radical molecules in vacuum. While green represents down spin, blue designates up spin density (SD), which dominates the surfaces.

Additionally, the current theoretical results are in good comparison with those of other antioxidants. For example, Hang and colleagues[22] have investigated the efficiency of the hydrogen scavenging process in some hydroxybenzoic acids at the M06-2X/6-311++G(d,p) level of quantum mechanics obtain values that vary from −24 to −41 kJ/mol for ΔBDE in aqueous solvent. At the same theoretical level, values of −59 and −53 kJ/mol have been reported for wedelolactone.[23] For licochalcone D studied at the B3LYP/6-311++G(d,p) level of quantum chemistry,[24] the differences are −36 and −25 kJ/mol in water solution. Furthermore, the two isoflavones outperform the other proposed antioxidant compounds. This is the case of para-

https://doi.org/10.1021/acs.jpca.3c05725
J. Phys. Chem. A 2023, 127, 10807−10816

Table 2. BDE and ΔBDE = $BDE_{molecule} - BDE_{phenol}$ Values (kJ/mol) Obtained by Using the ωB97XD/6-311++G(d,p) Level of Theory[a]

	gas phase		water		
bond	BDE	ΔBDE	BDE	ΔBDE	IC_{50} (μM)[32]
phenol exp	356−364[44−48]	n/a	369[49]	n/a	
phenol	361	0.0	358	0.0	
S10					72.2 ± 0.1
S10a	419	58	386	28	
S10b	373	12	364	6	
S10c	355	−6	334	−24	
S11					220.6 ± 0.1
S11a	418	57	386	28	
S11b	372	11	363	5	
S11c	356	−5	336	−22	
S11a′	418	57	386	28	
S11b′	373	−12	364	6	
S11c′	330	−31	331	−27	
<>V. guianensis<>					
leaf extract [μg mL^{-1}]					6.2 ± 0.4
sapwood extract [μg mL^{-1}]					3.7 ± 0.3

[a]The results in a water solvent, including those for phenol, are obtained using the polarizable-continuum model and experimental values of DPPH radical scavenging activity expressed as IC_{50} (50% inhibition concentration of DPPH assay).

trimerin, whose calculations of M05-2X/6-31+G(d) in the aqueous environment indicate ΔBDE of 25 kJ/mol, a poor description compared to phenol.[25]

3.2. SPLET Mechanism. The feasibility of the SPLET mechanism is considered by analyzing the PA and ETE that correspond to the viability of the compound to lose one proton and one electron in sequence. These results are shown in Table 3.

Table 3. Values for PA and ETE (kJ/mol) Were Estimated Using the Theory at the ωB97XD/6-311++G(d,p) Level

	PA		ETE		PA + ETE	
bond	gas phase	water	gas phase	water	gas phase	water
S10a	1460	164	275	350	1735	514
S10b	1380	116	308	375	1688	491
S10c	1449	153	221	308	1670	461
S11a	1463	163	270	350	1733	513
S11b	1382	116	305	375	1687	491
S11c	1458	155	213	309	1671	464

From the gas phase results, it can be seen that the SPLET mechanism is not a viable path. For example, for **S10**, the calculated PA value ranges from 1380 to 1460 kJ/mol. As these results are much higher than those reported for the HAT mechanism (355−419 kJ/mol), nature will prefer this last path to stabilize the hydrogen scavenging process. Table 3 states that similar conclusions are obtained for all **S11** radicals. Therefore, the SPLET mechanism does not occur in gaseous conditions.

On the other hand, in aqueous conditions, for the **S10** molecule, the results indicate PA values ranging from 116 to 164 kJ/mol, which is lower than those observed for the HAT mechanism (334−386 kJ/mol). This fact suggests that in a water solvent the compound prefers to lose a proton first. Once done, there is no alternative path other than losing the electron, which requires values ranging from 309 to 350 kJ/mol. Again, similar conclusions are made for all radicals **S11**. In summary, the solvent is not passive in hydrogen scavenging and acts by changing the route of the antioxidant from the gaseous medium to the solvent. Changes in the antioxidant mechanism from gas to solvent-mediated by the environment are often, and show the relevance of including environmental contributions if one is interested in quantifying the antioxidant behavior of compounds using quantum mechanics and thermochemical analysis.[55−60]

Table 3 also leads to other relevant conclusions. Among all of the possible radicals, **S10c** and **S11c** have the lowest energies in water. This fact indicates that hydrogen scavenging must occur at position *c* for both molecules. Consequently, it is concluded that the OH groups located in the chromone skeleton do not affect the antioxidant process. Furthermore, as can be seen, the sum PA + ETE is smaller for the radical **S10c** (461 kJ/mol) than for **S11c** (464 kJ/mol), suggesting that the first compound presents the best antioxidant activity.

3.3. SET-PT Mechanism. The last mechanism is SET-PT, which is described by the AIP and PDE shown in Table 4. As

Table 4. Values for AIP (kJ/mol) and PDE (kJ/mol) Were Computed Using Theory at the ωB97XD/6-311++G(d,p) Level

	AIP		PDE		AIP + PDE	
bond	gas phase	water	gas phase	water	gas phase	water
S10	708	459				
S10a			1027	55	1735	514
S10b			981	33	1689	492
S10c			962	3	1670	462
S11	708	460				
S11a			1025	54	1733	514
S11b			979	32	1687	492
S11c			963	4	1671	464

noted by the other two antioxidation mechanisms above, the sum of the AIP and PDE enthalpies indicates a scale like **S10a** > **S10b** > **S10c**, which means that the removal of hydrogen from position **S10c** must take precedence over the other two places. However, values ranging from 1670 to 1735 kJ/mol are observed in the gas phase, which is higher than the BDE parameters. The results are very similar for the molecule **S11**. Although the

https://doi.org/10.1021/acs.jpca.3c05725
J. Phys. Chem. A 2023, 127, 10807−10816

results confirm the enthalpy scale (**S11a** > **S11b** > **S11c**), the energies needed to stabilize this mechanism are still too high, ruling out this pathway.

3.4. Role of the Intramolecular HB Formation. Intramolecular HBs are relatively weak interactions that occur when an HB is formed inside the same molecule, commonly between hydrogen and a neighboring atom, such as oxygen, nitrogen, or fluorine, in the same molecule. This type of HB creates a weak but highly directional bond that can affect the various structural properties of the molecule. For example, the vibrational modes can be affected by intramolecular HB in several ways. The presence of an HB can alter the bonding strengths between atoms, resulting in changes in the vibrational frequencies, frequency shifts, and band intensity.[61] For this reason, the vibrational spectrum has been widely used to characterize the formation of HBs.

In principle, to understand the role of intramolecular H-bonds in antioxidant behavior, **S10** and **S11** should be considered as all the OH groups. However, from the experimental point of view, once positions a and b are the same for **S10** and **S11**, the origin of the differences in the antioxidant behavior comes from position c, which changes from one composition to another. Therefore, to better understand how hydrogen bonding acts, we decided to investigate another energetically possible structure (**S11′**) shown in Figure 2. Visually, the only difference from **S11** is the breaking of the intramolecular OH···CH_3 bond. However, the molecule **S11′** has an enthalpy of formation 24.45 kJ/mol higher than that calculated for **S11**.

Therefore, we will focus on O−H changes in the vibrational stretching mode and omitting the entire infrared plot. The results for absorption and intensity are reported in Table 5, in

Table 5. Vibrational Frequencies (cm^{-1}) and Intensities (km/mol) Corresponding to the O−H Stretching Mode of the Hydroxyl Group Involved in the Intramolecular HB OH···OCH_3

	gas phase		water	
compound	absorption	intensity	absorption	intensity
S10	3852.3	132.7	3828.9	224.2
S11	3857.8	134.1	3831.7	214.2
S11′	3917.6	119.9	3889.3	217.1

which significant solvent effects can be noted. For example, in gaseous conditions, a calculated vibrational frequency of 3852.3 cm^{-1} and an intensity of 132.7 km/mol are obtained, while in water, the results indicate a value of 3828.9 cm^{-1} associated with a 224.2 km/mol intensity. As can be seen, the solvent causes a bathochromic shift (−23.4 cm^{-1}) and a substantial intensity increase. The conclusions are similar for the **S11** molecule. Hence, from gas-to-solvent, a −26.1 cm^{-1} shift is obtained and a substantial increase in the intensity of this stretching mode.

To better understand the role of intramolecular HB formation, it is convenient to analyze the results obtained for the structure **S11′**, which is a minimal energy configuration that does not present an OH···OCH_3 intramolecular HB formation in the phenyl ring. With a frequency stretching of 3917.6 cm^{-1} a hypsochromic shift (59.8 cm^{-1}) is obtained concerning the original structure, **S11**, in the gas phase in addition to a decrease in the intensity of this vibrational mode. The same behavior is observed in water solvents in which the solvated **S11′** structure presents a hypsochromic shift of 57.5 cm^{-1} in the corresponding stretching mode for the **S11** conformation.

Even when we discuss the intramolecular coupling, it is worth noting that when moving horizontally in Table 5, a hypsochromic shift of about half of the previous one is observed, that is 28,3 for **S11′** and 26,1 for **S11**. Now, however, the intermolecular HBs are just grossly estimated by the PCM model. Therefore, consistent with the discussion presented above, there is no doubt that intramolecular HB affects the vibrational spectra of the compounds involved. On the other hand, the vibrational spectrum of a molecule provides information about the vibrational energies of the chemical bonds present, which are directly related to the enthalpy of the molecule.[61] Therefore, interactions such as intramolecular HB can influence the thermodynamic and reactive properties of the molecule. There are several initiatives in this direction.[62−64] In the gas phase, for example, these interactions vary from 8.37 to 62.76 kJ/mol,[61] which demands special attention once the values of ΔBDE, discussed above, generally exhibit the same order of magnitude of HB formation.[22−25] For example, from Table 2 in aqueous solution, it is possible to see that the BDE for the molecule **S10c** (334 kJ/mol) is slightly lower than that calculated for the radical **S11c** (336 kJ/mol), suggesting that **S10** is the best antioxidant compound. However, if the OH···OCH_3 HB structure is not allowed as in the **S11′c** molecule, a BDE value of 331 kJ/mol is obtained.

Although the **S11′** variant has the lowest BDE, nature prefers to favor the **S11** structure, which exhibits three intramolecular HBs with an enthalpy of −24.45 kJ/mol lower than **S11′**. Therefore, to correctly describe the antioxidant behavior of these molecules, it is essential to ensure the HB structures.

3.5. ICT Mechanism. HOMO−LUMO transition energies and SD are not antioxidant parameters like those mechanisms that define the HAT, SET-PT, and SPLET, but they do impact this property. The HOMO and LUMO (lower vacated molecular orbital) act as electron donor and acceptor sites, respectively. Furthermore, the HOMO−LUMO energy gap ($\Delta E = E_{LUMO} - E_{HOMO}$) indicates how difficult it is for electron excitation to occur from the valence to the conduction band. In Table 6, it can be seen that the compounds present a large

Table 6. Frontier Molecular Orbital Energies and Energy Gap Calculated for Molecules S10 and S11 Using the ωB97XD/6-311++G(d,p) Methods in Gas and Water (PCM)[a]

	gas phase			water		
compound	E_{HOMO}	E_{LUMO}	ΔE	E_{HOMO}	E_{LUMO}	ΔE
S10	−7.70	0.04	7.74	−7.85	−0.09	7.77
S11	−7.71	0.10	7.81	−7.85	−0.06	7.79

[a]All values are given in eV.

energy gap, respectively, −7.74 eV (**S10**) and −7.81 eV (**S11**). However, the permutation of the OH and OCH_3 groups has a slight impact on the electron structure of the compounds.

Furthermore, the LUMO distribution concentrated in the two fused rings indicates a possible ICT process in the fused ring system. To better understand this effect, we obtained the molecular dipole moment (μ) and the Mulliken charges (Q) in the Franck−Condon (FC) and ground state (GS). For the molecule **S10**, the calculations indicate values of 5.01 and 5.99 D, respectively, for μ_{GS} and μ_{FC}, suggesting a moderate charge redistribution. This statement is confirmed by counting the variation of the electric charges in the three molecular regions arranged in Figure 3b. From GS to FC, the red region of the molecule gains ΔQ_{S10} = −0.142 e from the yellow surfaces.

https://doi.org/10.1021/acs.jpca.3c05725
J. Phys. Chem. A 2023, 127, 10807−10816

Similar results are obtained for molecule **S11**. For this situation, μ_{GS} = 2.25 and μ_{FC} = 2.02 D, enough to generate a charge redistribution of $\Delta Q_{S11} = -0.112$ e bounded by the red surface. These statements confirm the effect of ICT on the **S10** and **S11** molecules.

4. CONCLUSIONS

We have systematically discussed the thermodynamics and radical hydrogen scavenging procedure of two new isoflavones initially isolated from *V. guianensis* leaves. Intramolecular dispersion effects are accounted for by the ωB97XD DFT method. Additionally, solvent contributions are accounted for using the standard PCM method.

An isoflavone is formed by attaching a chromone group to a phenol ring. Hence, regarding the molecular site where the hydrogen absorption process must occur, qualitative analysis of the frontier molecular orbitals and spin densities presents strong evidence that the phenol ring would be more susceptible to hydrogen subtraction. This statement is demonstrated by thermodynamic analysis of the three probable routes for radical formation (HAT, SPLET, and SET-PT). The results indicate that the HAT mechanism is energetically much more favorable in the gas phase. However, results in an aqueous environment indicate that polar solvents change the hydrogen elimination pathway to the SPLET mechanism. The inclusion of the effects of solvents is critical to understanding the experiment. The analysis of the enthalpies of formation suggests that the solvent better stabilizes the radicals formed.

Furthermore, the formation of intramolecular OH···OCH_3 HB in the phenolic ring provides ∼23 kJ/mol for structural stabilization, which is essential to describe the correct trend of antioxidant behavior, requiring special care if the conclusions come from molecular modeling approaches. In addition, the formation of intramolecular OH···OCH_3 HB in the phenolic ring contributes ∼23 kJ/mol for structural stabilization, which is essential to describe the correct trend of antioxidant behavior, requiring special care if the conclusions come from molecular modeling approximations.

The performance of these compounds is also available. The results indicate that both the molecules **S10** and **S11** exceed the estimates for phenol, which is a standard antioxidant compound, respectively, by −6 and −5 kJ/mol. However, concerning the phenol molecule, the solvent improves this performance to −24 and −22 kJ/mol. Furthermore, as the experiment indicates that **S10** would have the best antioxidant potential, these results confirm the expectation and reveal that the permutation of the OH and the OCH_3 groups controls this effect. In addition to unraveling the antioxidant mechanism of chromophores, the results suggest that these two isoflavones have potential use in the pharmacological and food industry.

AUTHOR INFORMATION

Corresponding Author

Rodrigo Gester − *Instituto de Física, Universidade de São Paulo, São Paulo, São Paulo 05588-090, Brazil; Faculdade de Física, Universidade Federal do Sul e Sudeste do Pará, Marabá, Pará 68507-590, Brazil;* orcid.org/0000-0001-6110-424X; Email: gester@unifesspa.edu.br

Authors

Sávio Fonseca − *Programa de Pós-Graduação em Química, Universidade Federal do Sul e Sudeste do Pará, Marabá, Pará 68507-590, Brazil;* orcid.org/0000-0003-1153-8749

Neidy S. S. dos Santos − *Programa de Pós-Graduação em Química, Universidade Federal do Sul e Sudeste do Pará, Marabá, Pará 68507-590, Brazil;* orcid.org/0000-0002-0177-8004

Alberto Torres − *Instituto de Física, Universidade de São Paulo, São Paulo, São Paulo 05588-090, Brazil*

Marcelo Siqueira − *Curso de Física, Universidade Federal do Amapá, Macapá, Amapá 68903-329, Brazil*

Antônio da Cunha − *Universidade Federal do Maranhão, Balsas, Maranhão CEP 65800-000, Brazil*

Vinícius Manzoni − *Instituto de Física, Universidade Federal de Alagoas, Maceió, Alagoas 57072-970, Brazil;* orcid.org/0000-0001-6779-3648

Patricio F. Provasi − *Department of Physics, IMIT, Northeastern University, Corrientes W3404 AAS, Argentina*

Sylvio Canuto − *Instituto de Física, Universidade de São Paulo, São Paulo, São Paulo 05588-090, Brazil;* orcid.org/0000-0002-9942-8714

Complete contact information is available at: https://pubs.acs.org/10.1021/acs.jpca.3c05725

Notes

The authors declare no competing financial interest.

ACKNOWLEDGMENTS

This study was financed in part by the Coordenação de Aperfeiçoamento de Pessoal de Nível Superior—Brasil (CAPES), Conselho Nacional de Desenvolvimento Científico e Tecnologico (CNPq), Fundação de Amparo à Pesquisa do Estado de São Paulo (FAPESP), Fundação de Amparo à Pesquisa e ao Desenvolvimento Científico e Tecnológico do Maranhão (FAPEMA), Fundação de Amparo à Pesquisa do Estado de Alagoas (FAPEAL), and Fundação de Amazônica de Amparo a Estudos e Pesquisas (FAPESPA). P.F.P. would like to acknowledge financial support from Consejo Nacional de Investigaciones Científicas y Técnicas (CONICET), PIP 11220200100467CO, and FaCENA-UNNE.

REFERENCES

(1) Sadiq, I. Z. Free Radicals and Oxidative Stress: Signaling Mechanisms, Redox Basis for Human Diseases, and Cell Cycle Regulation. *Curr. Mol. Med.* **2023**, *23*, 13−35.

(2) Alkadi, H. A Review on Free Radicals and Antioxidants. *Infect. Disord.: Drug Targets* **2020**, *20*, 16−26.

(3) Jesus, A.; Mota, S.; Torres, A.; Cruz, M. T.; Sousa, E.; Almeida, I. F.; Cidade, H. Honorina Cidade, Antioxidants in Sunscreens: Which and What For? *Antioxidants* **2023**, *12*, 138.

(4) Othón-Díaz, E. D.; Fimbres-García, J. O.; Flores-Sauceda, M.; Silva-Espinoza, B. A.; López-Martínez, L. X.; Bernal-Mercado, A. T.; Ayala-Zavala, J. F. Antioxidants in Oak (Quercus sp.): Potential Application to Reduce Oxidative Rancidity in Foods. *Antioxidants* **2023**, *12*, 861.

(5) Pruteanu, L. L.; Bailey, D. S.; Grădinaru, A. C.; Jäntschi, L. The Biochemistry and Effectiveness of Antioxidants in Food, Fruits, and Marine Algae. *Antioxidants* **2023**, *12*, 860.

(6) Marino, P.; Pepe, G.; Basilicata, M. G.; Vestuto, V.; Marzocco, S.; Autore, G.; Procino, A.; Gomez-Monterrey, I. M.; Manfra, M.; Campiglia, P. Potential Role of Natural Antioxidant Products in Oncological Diseases. *Antioxidants* **2023**, *12*, 704.

(7) Alagona, G.; Ghio, C. Antioxidant Properties of Pterocarpans through Their Copper(II) Coordination Ability. A DFT Study in Vacuo and in Aqueous Solution. *J. Phys. Chem. A* **2009**, *113*, 15206−15216.

(8) de Souza, G. L. C.; Peterson, K. A. Benchmarking Antioxidant-Related Properties for Gallic Acid through the Use of DFT, MP2,

CCSD, and CCSD(T) Approaches. *J. Phys. Chem. A* **2021**, *125*, 198−208.
(9) Wang, Z.; Gao, X.; Zhao, Y. Mechanisms of Antioxidant Activities of Fullerenols from First-Principles Calculation. *J. Phys. Chem. A* **2018**, *122*, 8183−8190.
(10) Nenadis, N.; Pyrka, I.; Tsimidou, M. Z. The Contribution of Theoretical Prediction Studies to the Antioxidant Activity Assessment of the Bioactive Secoiridoids Encountered in Olive Tree Products and By-Products. *Molecules* **2023**, *28*, 2267.
(11) Gui, H.; Dai, J.; Tian, J.; Jiang, Q.; Zhang, Y.; Ren, G.; Song, B.; Wang, M.; Saiwaidoula, M.; Dong, W.; et al. The isolation of anthocyanin monomers from blueberry pomace and their radical-scavenging mechanisms in DFT study. *Food Chem.* **2023**, *418*, 135872.
(12) Yusuff, O. K.; Abdul Raheem, M. A. O.; Mukadam, A. A.; Sulaimon, R. O. Kinetics and Mechanism of the Antioxidant Activities of C. olitorius and V. amygdalina by Spectrophotometric and DFT Methods. *ACS Omega* **2019**, *4*, 13671−13680.
(13) de Souza, G. L. C.; Peterson, K. A. Benchmarking Antioxidant-Related Properties for Gallic Acid through the Use of DFT, MP2, CCSD, and CCSD(T) Approaches. *J. Phys. Chem. A* **2021**, *125*, 198−208.
(14) Abuelizz, H. A.; Taie, H. A. A.; Bakheit, A. H.; Mostafa, G. A. E.; Marzouk, M.; Rashid, H.; Al-Salahi, R. Investigation of 4-Hydrazinobenzoic Acid Derivatives for Their Antioxidant Activity: In Vitro Screening and DFT Study. *ACS Omega* **2021**, *6*, 31993−32004.
(15) Xue, Y.; Zheng, Y.; An, L.; Dou, Y.; Liu, Y. Density functional theory study of the structure−antioxidant activity of polyphenolic deoxybenzoins. *Food Chem.* **2014**, *151*, 198−206.
(16) Azevedo, J.; Oliveira, J.; Cruz, L.; Teixeira, N.; Brás, N. F.; de Freitas, V.; Mateus, N. Antioxidant Features of Red Wine Pyranoanthocyanins: Experimental and Theoretical Approaches. *J. Agric. Food Chem.* **2014**, *62*, 7002−7009.
(17) Tiwari, M. K.; Mishra, P. C. Anti-oxidant activity of 6-gingerol as a hydroxyl radical scavenger by hydrogen atom transfer, radical addition and electron transfer mechanisms. *J. Chem. Sci.* **2016**, *128*, 1199−1210.
(18) Djafarou, S.; Boulebd, H. The radical scavenger capacity and mechanism of prenylated coumestan-type compounds: a DFT analysis. *Free Radical Res.* **2022**, *56*, 273−281.
(19) Urbaniak, A.; Szeląg, M.; Molski, M. Theoretical investigation of stereochemistry and solvent influence on antioxidant activity of ferulic acid. *Comput. Theor. Chem.* **2013**, *1012*, 33−40.
(20) Urbaniak, A.; Kujawski, J.; Czaja, K.; Szelag, M. Antioxidant properties of several caffeic acid derivatives: A theoretical study. *C. R. Chim.* **2017**, *20*, 1072−1082.
(21) McQuarrie, D..; Simon, J.. *Molecular Thermodynamics*; University Science Books: Sausalito, CA, 1999.
(22) Hang, D. T. N.; Hoa, N. T.; Bich, H. N.; Mechler, A.; Vo, Q. V. The hydroperoxyl radical scavenging activity of natural hydroxybenzoic acids in oil and aqueous environments: Insights into the mechanism and kinetics. *Phytochemistry* **2022**, *201*, 113281.
(23) Chen, M.; Li, Z.; Sun, G.; Jin, S.; Hao, X.; Zhang, C.; Liu, L.; Zhang, L.; Liu, H.; Xue, Y. Theoretical study on the free radical scavenging potency and mechanism of natural coumestans: Roles of substituent, noncovalent interaction and solvent. *Phytochemistry* **2023**, *207*, 113580.
(24) Mittal, A.; Kakkar, R. The antioxidant potential of retrochalcones isolated from liquorice root: A comparative DFT study. *Phytochemistry* **2021**, *192*, 112964.
(25) Ngo, T. C.; Mai, T. V.-T.; Pham, T. T.; Jeremic, S.; Markovic, Z.; Huynh, L. K.; Dao, D. Q. Natural acridones and coumarins as free radical scavengers: Mechanistic and kinetic studies. *Chem. Phys. Lett.* **2020**, *746*, 137312.
(26) Pammi, S. S. S.; Suresh, B.; Giri, A. Antioxidant potential of medicinal plants. *J. Crop Sci. Biotechnol.* **2023**, *26*, 13−26.
(27) Pietta, P. G. Flavonoids as Antioxidants. *J. Nat. Prod.* **2000**, *63*, 1035−1042.
(28) Rice-Evans, C. Flavonoid Antioxidants. *Med. Chem.* **2001**, *8*, 797−807.
(29) Ma, E. Z.; Khachemoune, A. Flavonoids and their therapeutic applications in skin diseases. *Arch. Dermatol. Res.* **2022**, *315*, 321−331.
(30) Li, M.; Qian, M.; Jiang, Q.; Tan, B.; Yin, Y.; Han, X. Evidence of Flavonoids on Disease Prevention. *Antioxidants* **2023**, *12*, 527.
(31) Souza, R. F.; da Silva, G. A.; Arruda, A. C.; da Silva, M. N.; Santos, A. S.; Grisólia, D.; Silva, M. B.; Salgado, C. G.; Arruda, M. S. A New Prenylisoflavone from the Antifungal Extract of Leaves of Vatairea guianensis Aubl. *J. Braz. Chem. Soc.* **2016**, *28*, 1132−1136.
(32) de Souza, R. F.; Arruda, M. S. P.; *Estudo químico e avaliação de atividades biológicas da espécie Vatairea guianensis AUBL. (FABACEAE)*. Ponta Grossa (PR); Atena Ed.a, 2017; p 157.
(33) Parr, R. G.; Yang, W. *Density Functional Theory of Atoms and Molecules*; Oxford Science Publications, 1994.
(34) Hohenberg, P.; Kohn, W. Inhomogeneous Electron Gas. *Phys. Rev.* **1964**, *136*, B864−B871.
(35) Kohn, W.; Sham, L. J. Self-Consistent Equations Including Exchange and Correlation Effects. *Phys. Rev.* **1965**, *140*, A1133−A1138.
(36) Chai, J.-D.; Head-Gordon, M. Long-range corrected hybrid density functionals with damped atom-atom dispersion corrections. *Phys. Chem. Chem. Phys.* **2008**, *10*, 6615.
(37) Clark, T.; Chandrasekhar, J.; Spitznagel, G. W.; Schleyer, P. v.R. Efficient diffuse function-augmented basis sets for anion calculations. III. The 3-21+G basis set for first-row elements, Li-F. *J. Comput. Chem.* **1983**, *4*, 294−301.
(38) Krishnan, R.; Binkley, J. S.; Seeger, R.; Pople, J. A. Self-consistent molecular orbital methods. XX. A basis set for correlated wave functions. *J. Chem. Phys.* **1980**, *72*, 650−654.
(39) Miertuš, S.; Scrocco, E.; Tomasi, J. Electrostatic Interaction of a Solute with a Continuum. A Direct Utilization of ab initio Molecular Potentials for the Prevision of Solvent Effects. *Chem. Phys.* **1981**, *55*, 117.
(40) Frisch, M. J.; et al. *Gaussian 09*, Revision A.02; Gaussian Inc: Wallingford CT, 2016.
(41) Cabral, B. J. C.; Canuto, S. The enthalpy of the O−H bond homolytic dissociation: Basis-set extrapolated density functional theory and coupled cluster calculations. *Chem. Phys. Lett.* **2005**, *406*, 300−305.
(42) Cabral, B. J. C.; Canuto, S. Reply to comment on 'The enthalpy of the O−H bond homolytic dissociation: Basis-set extrapolated density functional theory and coupled cluster calculations. *Chem. Phys. Lett.* **2006**, *417*, 570−572.
(43) Lu, T.; Chen, F. Multiwfn: A multifunctional wavefunction analyzer. *J. Comput. Chem.* **2012**, *33*, 580−592.
(44) Mulder, P.; Saastad, O. W.; Griller, D. Oxygen-hydrogen bond dissociation energies in para-substituted phenols. *J. Am. Chem. Soc.* **1988**, *110*, 4090−4092.
(45) DeFrees, D. J.; McIver, R. T.; Hehre, W. J. Heats of formation of gaseous free-radicals via ion-cyclotron double-resonance spectroscopy. *J. Am. Chem. Soc.* **1980**, *102*, 3334−3338.
(46) Colussi, A. J.; Zabel, F.; Benson, S. W. The very low-pressure pyrolysis of phenyl ethyl ether, phenyl allyl ether, and benzyl methyl ether and the enthalpy of formation of the phenoxy radical. *Int. J. Chem. Kinet.* **1977**, *9*, 161−178.
(47) Walker, J. A.; Tsang, W. Single-pulse shock tube studies on the thermal decomposition of n-butyl phenyl ether, n-pentylbenzene, and phenetole and the heat of formation of phenoxy and benzyl radicals. *J. Phys. Chem.* **1990**, *94*, 3324−3327.
(48) Arends, I. W.; Louw, R.; Mulder, P. J. Kinetic study of the thermolysis of anisole in a hydrogen atmosphere. *J. Phys. Chem.* **1993**, *97*, 7914−7925.
(49) Lind, J.; Shen, X.; Eriksen, T. E.; Merenyi, G. The one-electron reduction potential of 4-substituted phenoxyl radicals in water. *J. Am. Chem. Soc.* **1990**, *112*, 479−482.
(50) Chen, J.; Yang, J.; Ma, L.; Li, J.; Shahzad, N.; Kim, C. K. Structure-antioxidant activity relationship of methoxy, phenolic hydroxyl, and carboxylic acid groups of phenolic acids. *Sci. Rep.* **2020**, *10*, 2611.
(51) Chen, Z.; Bertin, R.; Froldi, G. EC50 estimation of antioxidant activity in DPPH assay using several statistical programs. *Food Chem.* **2013**, *138*, 414−420.

https://doi.org/10.1021/acs.jpca.3c05725
J. Phys. Chem. A 2023, 127, 10807−10816

(52) Zuo, G.-Y.; Yang, C.-X.; Han, J.; Li, Y. Q.; Wang, G. C. Synergism of prenylflavonoids from Morus alba root bark against clinical MRSA isolates. *Phytomedicine* **2018**, *39*, 93−99.
(53) Bustos, P. S.; Deza-Ponzio, R.; Páez, P. L.; Cabrera, J. L.; Virgolini, M. B.; Ortega, M. G. Flavonoids as protective agents against oxidative stress induced by gentamicin in systemic circulation. Potent protective activity and microbial synergism of luteolin. *Food Chem. Toxicol.* **2018**, *118*, 294−302.
(54) Vivek, T.; Lokhande, M. N. Chapter 9-Compound synergy in natural crude extract: a novel concept in drug formulation. *Progess in Biochemistry and Biotechnology*, New Horizons in Natural Compound Research; Meena, S. N., Nandre, V., Kodam, K., Meena, R. S. Academic Press, 2023; pp 167−178.
(55) Spiegel, M.; Cel, K.; Sroka, Z. The mechanistic insights into the role of pH and solvent on antiradical and prooxidant properties of polyphenols — Nine compounds case study. *Food Chem.* **2023**, *407*, 134677.
(56) Chen, M.; Li, Z.; Sun, G.; Jin, S.; Hao, X.; Zhang, C.; Liu, L.; Zhang, L.; Liu, H.; Xue, Y. Theoretical study on the free radical scavenging potency and mechanism of natural coumestans: Roles of substituent, noncovalent interaction and solvent. *Phytochemistry* **2023**, *207*, 113580.
(57) Wang, G.; Liu, Y.; Zhang, L.; An, L.; Chen, R.; Liu, Y.; Luo, Q.; Li, Y.; Wang, H.; Xue, Y. Computational study on the antioxidant property of coumarin-fused coumarins. *Food Chem.* **2020**, *304*, 125446.
(58) Zheng, Y.-Z.; Deng, G.; Guo, R.; Fu, Z.-M.; Chen, D.-F. The influence of the H5···O C4 intramolecular hydrogen-bond (IHB) on the antioxidative activity of flavonoid. *Phytochemistry* **2019**, *160*, 19−24.
(59) Zheng, Y.-Z.; Chen, D.-F.; Deng, G.; Guo, R.; Fu, Z.-M. The antioxidative activity of piceatannol and its different derivatives: Antioxidative mechanism analysis. *Phytochemistry* **2018**, *156*, 184−192.
(60) Zheng, Y.-Z.; Deng, G.; Chen, D.-F.; Liang, Q.; Guo, R.; Fu, Z.-M. Theoretical studies on the antioxidant activity of pinobanksin and its ester derivatives: Effects of the chain length and solvent. *Food Chem.* **2018**, *240*, 323−329.
(61) Scheiner, S. *Hydrogen Bonding: A Theoretical Perspective*, 1st ed.; Oxford University Press: New York, USA, 1977.
(62) Zheng, Y.-Z.; Fu, Z.-M.; Deng, G.; Guo, R.; Chen, D.-F. Role of C-H bond in the antioxidant activities of rooperol and its derivatives: A DFT study. *Phytochemistry* **2020**, *178*, 112454.
(63) Shang, C.; Zhang, Y.; Sun, C.; Wang, L. Tactfully improve the antioxidant activity of 2'-hydroxychalcone with the strategy of substituent, solvent and intramolecular hydrogen bond effects. *J. Mol. Liq.* **2022**, *362*, 119748.
(64) Zheng, Y.-Z.; Zhou, Y.; Liang, Q.; Chen, D.-F.; Guo, R.; Xiong, C.-L.; Xu, X.-J.; Zhang, Z.-N.; Huang, Z.-J. Solvent effects on the intramolecular hydrogen-bond and anti-oxidative properties of apigenin: A DFT approach. *Dyes Pigm.* **2017**, *141*, 179−187.

https://doi.org/10.1021/acs.jpca.3c05725
J. Phys. Chem. A 2023, 127, 10807−10816